Localized States in 1D Frenkel Exciton Systems: A Comparison between Infinite-Range and Nearest-Neighbor Transfer for Normal and Inverted Bands

ARTICLE *in* THE JOURNAL OF PHYSICAL CHEMISTRY B · SEPTEMBER 2009

Impact Factor: 3.3 · DOI: 10.1021/jp9061863 · Source: PubMed

2 AUTHORS:

I. Avgin
Ege University
41 PUBLICATIONS **147** CITATIONS
SEE PROFILE

David Lawrence Huber
University of Wisconsin–Madison
93 PUBLICATIONS **788** CITATIONS
SEE PROFILE

Localized States in 1D Frenkel Exciton Systems: A Comparison between Infinite-Range and Nearest-Neighbor Transfer for Normal and Inverted Bands

I. Avgin

Department of Electrical and Electronics Engineering, Ege University, Bornova 35100, Izmir, Turkey

D. L. Huber

Department of Physics, University of Wisconsin-Madison, Madison, Wisconsin 53706

Received: July 1, 2009; Revised Manuscript Received: August 12, 2009

We investigate localized states in one-dimensional Frenkel exciton systems that are created by a shift in the optical transition frequency of a single chromophore. In this paper, we focus on localized states lying below the exciton band that can act as exciton traps. A comparison is made between systems with infinite-range (r^{-n}, $n = 2, 3, ...$) transfer and those with nearest-neighbor ($n = \infty$) transfer. A distinction is also made between normal bands (minimum exciton energy at $k = 0$) and inverted bands (minimum energy at $k = \pi$). The position of the localized state relative to the bottom of the band is calculated as a function of the shift in the single-chromophore transition frequency. The nature of the localized state is displayed in calculations of the participation ratio and the effective oscillator strength. Similarities and differences in localized states between normal and inverted band systems and between infinite-range and nearest-neighbor transfer are analyzed.

I. Introduction

Broadly speaking, the transport of optical excitation in nonmetallic crystalline systems is generally divided into two categories: incoherent transfer where the localized excitation hops (or diffuses) from site to site in a thermally activated process and coherent transfer in which the relevant excited states are excitons that under ideal conditions propagate as coherent waves. In this article, we focus on the latter. Both incoherent and coherent transfer are affected by traps, which are low-lying localized states that capture the excitation and remove it from the transfer process. When kT is much greater than the trap depth, the excitation can be thermally excited back to the conducting state, provided the lifetime in the trapped state is long in comparison with the back-transfer rate. If the back-transfer takes place relatively slowly, the trapped state can either fluoresce or undergo nonradiative decay.

In this article, we investigate conditions for formation and other properties of localized states in 1D systems where the optically active excited states are Frenkel excitons.[1] The starting point is the Frenkel Hamiltonian for an ideal array of chromophores:

$$H_0 = E_0 \sum_j |j><j| - \sum_{(j,j')} T_{jj'}(|j><j'| + |j'><j|) \quad (1)$$

where E_0 is the chromophore transition frequency and the $T_{jj'}$ are the transfer integrals, which depend only on the relative separation of sites j and j'. The first sum is over the N ($N \gg 1$) sites in the array, and the second sum is over all (j,j') pairs for which the transfer integral is nonzero. In 1D, the energy levels of this Hamiltonian take the form (assuming periodic boundary conditions)

$$e(k) = E_0 - \sum_{j'} T_{jj'} \cos [k(j - j')] \quad (2)$$

where the sum on j' is over all sites for which $T_{jj'}$ is nonzero. The wave vector k is confined to the first Brillouin zone of the chromophore lattice, and the unit of length is the lattice constant so that $-\pi \leq k \leq \pi$. In our calculations, the trap is associated with a site where the chromophore transition frequency has a value that differs from the corresponding value in the unperturbed system.

The approach we will follow was first employed by Koster and Slater in connection with impurity states in electronic band structures.[2] Analogous techniques were used to analyze the effect of an impurity atom on the vibrational spectra of a solid by Montroll and Potts[3] and subsequently by Mahanty, Maradudin, and Weiss.[4] The same approach can also be utilized to characterize spin-wave impurity states in ferromagnets as shown by Wolfram and Callaway.[5] Recently, similar techniques were used by us to characterize localized states in π-conjugated polymers that are induced by abrupt changes in the torsion angle between adjacent monomers.[6] As shown in refs 1−6, one can utilize operator techniques to rewrite the Schrödinger equation in the form

$$(I - G_0(E)H_1)|\Psi> = 0 \quad (3)$$

where $|\Psi>$ is the eigenstate associated with the eigenvalue E:

$$|\Psi> = \sum_j |j> a_j \quad (4)$$

with $|j>$ being a state where the jth chromophore is excited, all others being in the ground state, and a_j is the corresponding

10.1021/jp9061863 CCC: $40.75
Published on Web 09/29/2009

amplitude. The symbol H_1 denotes the Hamiltonian associated with the perturbed site and G_0 is the Green's operator $G_0(E) = (E - H_0)^{-1}$, where H_0 is the unperturbed Hamiltonian.

In the case where the perturbation consists only of the shift of the transition frequency of a single chromophore, that is $E_0 \rightarrow E_0 + 2\varepsilon$, the eigenvalue equation reduces to the simple form

$$2\varepsilon g_0(E) = 1 \tag{5}$$

where $g_0(E)$ is a lattice Green's function. In 1D, the lattice Green's functions are defined by the equation

$$g_j(E) = \pi^{-1} \int_0^{\pi} \mathrm{d}k \cos(jk)(E - e(k))^{-1} \tag{6}$$

when the defect is located at site $j = 0$. The eigenvectors, or site amplitudes, associated with a localized state of energy E_v can be expressed as

$$a_{vj} = C g_j(E_v) \tag{7}$$

where C is a normalization constant and g_j is the lattice Green's function defined in eq 6.

The essential components of the analysis are displayed in eqs 2 and eqs 5−7. Eq 5 is an eigenvalue equation that gives the energy of the localized state as a function of the shift in the transition frequency. It involves the lattice Green's function, $g_0(E)$, defined in eq 6. The Green's function, in turn, is determined by the exciton energy in the ideal system (eq 2). The amplitude of the of the localized state wave function on site j of the 1D lattice is given by eq 7 where it is seen to be proportional to the lattice Green's function $g_j(E)$. It should be noted that the Green's function approach reduces the determination of the energy and wave function of the localized state to the calculation of the unperturbed exciton energy $e(k)$ (a direct summation) and the subsequent evaluation of the 1D integrals defining the Green's functions. This is a great simplification over the approach based on matrix diagonalization. In the case of infinite-range interactions, which is the primary focus of this investigation, the simplification is present only for perturbations in the transition frequency. The investigations of the effects of perturbations in the transfer integrals (so-called off-diagonal perturbations) generally require diagonalizing $N \times N$ matrices, where N is the number of sites in the lattice.

We are interested in the solution to eq 5 in trapping situations, that is the localized state is below the bottom of the exciton band, a configuration that occurs when $\varepsilon < 0$. We consider both normal bands (zone center state lowest in energy) and inverted bands (zone edge state lowest in energy). Note that the localized states below the band in the inverted system ($\varepsilon < 0$) correspond to states above the band in the equivalent normal system with shift equal to $2|\varepsilon|$. In section II, we review previous results for nearest-neighbor transfer, typically associated with exchange processes involving wave function overlap, and define certain functions that characterize the properties of the eigenfunctions, whereas, in section III, we present results for infinite-range transfer of the form $T_{jj'} \propto |x_j - x_{j'}|^{-n}$, including the physically relevant electric dipole−dipole transfer ($n = 3$), and compare them with the nearest-neighbor findings. Section IV contains a brief discussion of our results along with comments on their implications for real materials. Some of the mathematical details of the analysis of the model system where $n = 2$ are covered in the Appendix.

II. Nearest-Neighbor Transfer

In 1D with the nearest-neighbor transfer integral $T_{j,j+1}$ equal to 1, the exciton energy is expressed as $e(k) = -2 \cos k$ for normal bands and $e(k) = 2 \cos k$ for inverted bands, whereas the Green's function $g_0(E)$ reduces to $\pm(E^2 - 4)^{-1/2}$ for $|E| > 2$, with the sign depending on whether E is positive or negative. With negative ε, the localized state lies below the bottom of the band and have the energy $-2(1 + \varepsilon^2)^{1/2}$ for both normal and inverted bands.

Next, we consider the wave functions of the localized states. To characterize their spatial extent, we use the participation ratio (PR) defined by[7]

$$\mathrm{PR}(\nu) = (\sum_j |a_{\nu j}|^2)^2 / \sum_j |a_{\nu j}|^4 \tag{8}$$

where $a_{\nu j}$, the amplitude of eigenstate ν on site j is given by eq 7. Note that PR = 1 for an eigenstate localized on a single site, PR = N for a delocalized state in a defect-free chain of N sites with periodic boundary conditions, whereas, in general, PR is a measure of the number of sites where the state ν has significant amplitude.

In the case of nearest-neighbor transfer the Green's functions take the form[6,7]

$$g_j(E) = E^{-1}(1 - 4/E^2)^{-1/2}[(E/2)\{(1 - 4/E^2)^{1/2} - 1\}]^{|j|} \tag{9}$$

From eq 9 it is evident that the Green's functions provide a direct connection between the energy of the localized state and the corresponding site amplitudes.

In the case of nearest-neighbor transfer, the participation ratio for a localized state with energy E_{loc} is given by[7]

$$\mathrm{PR}(E_{\mathrm{loc}}) = (1 + x_{\mathrm{loc}}^2)^3 / [(1 - x_{\mathrm{loc}}^2)(1 + x_{\mathrm{loc}}^4)] \tag{10}$$

where

$$x_{\mathrm{loc}} = (E_{\mathrm{loc}}/2)[(1 - 4/E_{\mathrm{loc}}^2)^{1/2} - 1] \tag{11}$$

We can gain some insight into the relative optical activity of the localized states from the effective oscillator strength (EOS) defined by[6]

$$\mathrm{EOS}(\nu) = |\sum_j a_{\nu j}|^2 / \sum_j |a_{\nu j}|^2 \tag{12}$$

The EOS is the square of a dimensionless transition dipole moment for a system where the dipole moment of the perturbed site is the same as the moment of a site in the ideal array. Just as with the participation ratio, the EOS can be easily evaluated for a system with nearest-neighbor transfer with the result[7]

$$\mathrm{EOS}(x_{\mathrm{loc}}) = (1 + x_{\mathrm{loc}})^3 / [(1 - x_{\mathrm{loc}})((1 + x_{\mathrm{loc}}^2)] \tag{13}$$

where x_{loc} is given by eq 11.

It should be noted that the approximation of identical dipole moments can be easily circumvented by weighting the contribution of the defect site ($j = 0$) in numerator in eq 12 by the ratio of the perturbed dipole moment to the unperturbed moment. In a situation where the localized state lies near the bottom of the band (and thus the localized state wave function decays slowly with distance from the defect), the perturbation in the dipole moment has little effect on the EOS because the dominant contribution comes from the unperturbed sites. In contrast, in the opposite limit, where the localized state lies well below the band edge, the localized state wave function decays rapidly, and the dipole moment of the defect site makes a relatively larger contribution to the EOS.

In the following section, we will compare the results for nearest-neighbor transfer that are presented above with similar results obtained from systems with infinite-range transfer.

III. Infinite-Range Interactions

A. 1D Model Calculation. The conditions for localized states in 1D are more restrictive with infinite-range interactions. To show this, we first investigate a simple model where the calculations can be carried out analytically. We consider a system where the transfer integral connecting sites j and j' is $-|j - j'|^{-2}$ and is thus equal to 1 when the sites are nearest-neighbors. The exciton energy is then given by[8]

$$e(k) = \pm\left(\frac{\pi^2}{6} - \frac{(k - \pi)^2}{2}\right) \tag{14}$$

where the + sign refers to the normal band, with lower band edge at $-\pi^2/3$, and the − sign to the inverted band with lower band edge at $-\pi^2/6$. The corresponding lattice Green's function is expressed as

$$g_0(E) = \frac{\pi^{-1}}{(\pi^2/3 - 2E)^{1/2}} \ln\left(\frac{(\pi^2/3 - 2E)^{1/2} - \pi}{(\pi^2/3 - 2E)^{1/2} + \pi}\right) \tag{15}$$

for the normal band with $E < -\pi^2/3$ and

$$g_0(E) = \frac{-2/\pi}{(-2E - \pi^2/3)^{1/2}} \tan^{-1}\left(\frac{\pi}{(-2E - \pi^2/3)^{1/2}}\right) \tag{16}$$

for the inverted band with $E < -\pi^2/6$.

Employing eq 5, along with eqs 15 and 16, yields expressions for the energy of the localized states as a function of ε. In the case of the inverted band, the energy of the localized state near the bottom of the band is $-\pi^2/6 - 2\varepsilon^2$ because the arctan function in (16) is approximately $\pi/2$. With the normal band, the radical in eq 15 near the band edge is approximately equal to $\pi + \Delta/\pi$ where $\Delta = -\pi^2/3 - E_{loc}$ so that when $\varepsilon < 0$, the equation for the localized state energy reduces to

$$2\varepsilon\pi^{-2} \ln(\Delta/2\pi^2) = 1 \tag{17}$$

From this equation, it is evident that the energy of the localized state relative to the bottom of the band varies as $2\pi^2 \exp[-\pi^2/2|\varepsilon|]$. In contrast, the energy of the localized state for the inverted band varies as $-2\varepsilon^2$ relative to the bottom of the band, which is qualitatively similar to the variation found in 1D systems with finite range transfer. The asymptotic variation of the amplitudes of the localized states is treated in the Appendix where it is shown that in the case of normal bands, when $\Delta/\pi^2 \ll 1$, the amplitude on site j varies as $-(j\Delta)^{-2}$ in the limit $j \to \infty$. With inverted bands, the asymptotic amplitude varies exponentially as $-(2\Lambda)^{-1/2} \cos(j\pi) \exp[-j(2\Lambda)^{1/2}]$, where $\Lambda = -\pi^2/6 - E_{loc}$. The latter behavior is similar to the behavior found for 1D systems with nearest-neighbor transfer.

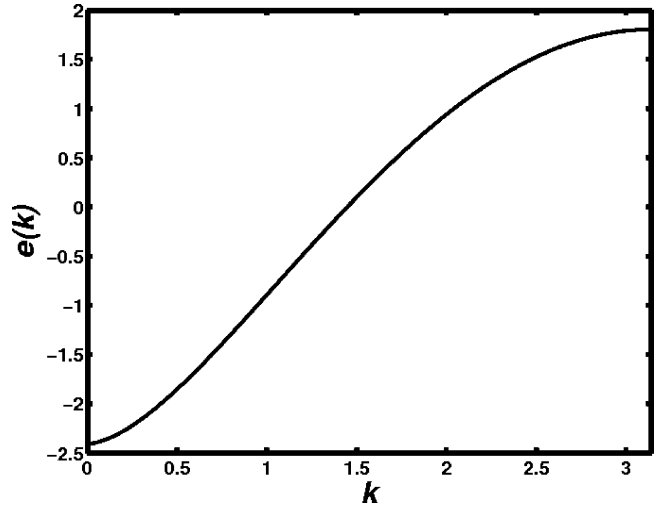

Figure 1. Exciton energy $e(k)$ vs k, $0 \le k \le \pi$, for a normal band with dipole−dipole transfer, $T_{jj'} = -|j-j'|^{-3}$.

B. 1D-Dipole−Dipole Transfer. In the case of $n = 3$ (a realistic model for electric dipole−dipole transfer), the band edges can be expressed in terms of the Riemann zeta function $\zeta(3)$.[9] When the transfer integral between sites j and j' is written $-|j - j'|^{-3}$, the lower edge for a normal band is at $-2\zeta(3) = -2.4041$ ..., whereas the upper band edge is at $(3/2)\zeta(3) = 1.8030$; in the case of the inverted band, the lower edge is at $-(3/2)\zeta(3)$ and the upper edge at $2\zeta(3)$. We use standard numerical techniques to calculate $e(k)$, with the results for the normal band shown in Figure 1 for $0 \le k \le \pi$. The Green's functions are then obtained by direct integration using the numerical results for $e(k)$.

C. Comparison between Infinite-Range and Nearest-Neighbor Transfer. In Figure 2, we show the results for the variation in the energy of the localized state relative to the bottom of the band versus $|\varepsilon|$. The upper dashed and solid curves refer to inverted band systems with $n = 2$ and 3 respectively, whereas the lower dashed and solid curves are for normal band systems, with $n = 2$ and 3, respectively. The broken curve in the middle is the result for both normal and inverted bands in a system with nearest-neighbor transfer, $2(1 + \varepsilon^2)^{1/2} - 2$. Particularly noteworthy is the relatively weak dependence on $|\varepsilon|$ for the infinite-range, normal-band systems, especially for $n = 2$.

In Figure 3, we display the results for the participation ratio (PR) versus the absolute value of the energy of the localized state relative to the bottom of the band. The labeling of the curves is the same as in Figure 2. It should be noted that the curves for $n = 2$ and $n = 3$ for the normal band are nearly identical as are the curves for the nearest-neighbor normal band (which is the same as the curve for nearest-neighbor inverted band) and the $n = 2$ and $n = 3$ inverted bands, with the latter being nearly coincident with the nearest-neighbor results. The equality of the participation ratios for the normal and inverted nearest-neighbor bands is a direct consequence of the fact that the amplitude of a localized state of a given energy in the

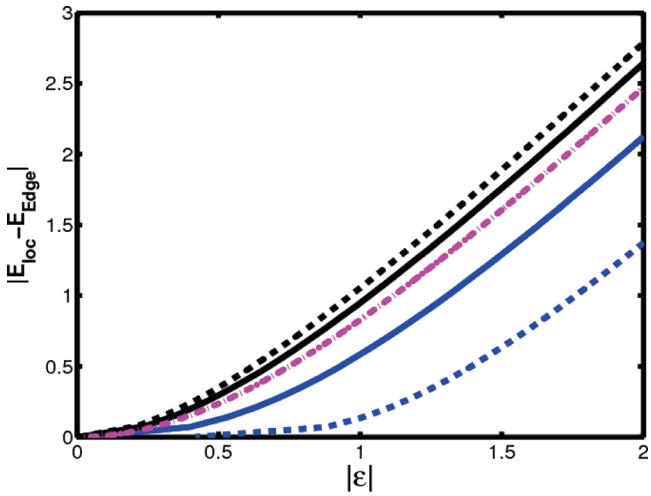

Figure 2. Energy of the localized states relative to the lower band edge vs $|\varepsilon|$. From top to bottom, the curves correspond to inverted band, $n = 2$; inverted band, $n = 3$; inverted and normal bands, nearest-neighbor transfer; normal band, $n = 3$; normal band, $n = 2$. Energy is in units of the nearest-neighbor transfer integral.

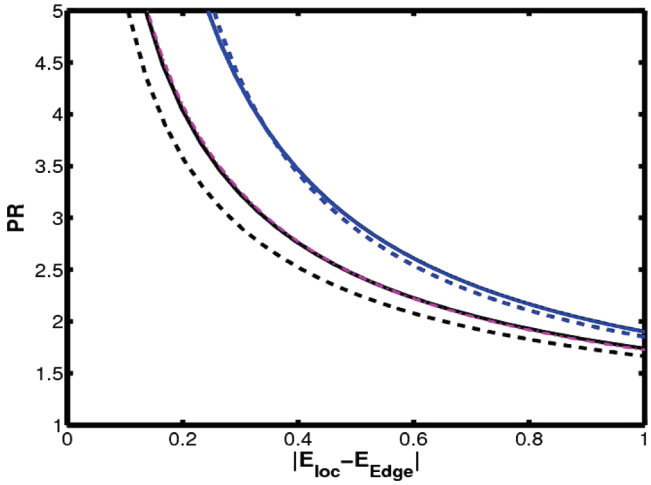

Figure 3. Participation ratio (PR) vs energy of the localized states relative to the bottom of the band. From left to right: dashed curve, inverted band, $n = 2$; solid curve, inverted band, $n = 3$, broken curve (nearly coincident with inverted band, $n = 3$), nearest-neighbor with identical results for normal and inverted bands; solid curve, normal band, $n = 3$; dashed curve, normal band, $n = 2$. Energy is in units of the nearest-neighbor transfer integral. Data displayed in the nearest-neighbor curve are obtained from eq 10.

inverted band case differs only by the phase factor $\cos(j\pi)$ from the corresponding state in the normal-band counterpart when the defect is located at the site $j = 0$. Note that, in all cases, the PR diverges as the localized state approaches the band edge.

The results for the effective oscillator strength (EOS) are displayed in Figure 4. The upper three curves refer to the normal bands, whereas the lower three curves show the results for the inverted bands. The EOS for the normal bands diverge as the localized state approaches the band edge, similar to the PR. In contrast, the EOS for the inverted bands approaches zero in the same limit. The qualitative distinction between the normal and inverted bands is a direct consequence of the fact that the amplitudes for the inverted bands oscillate in sign symmetrically about the site of the impurity, whereas the amplitudes for the normal bands decrease monotonically with distance from the impurity (see eq 9 for nearest-neighbor results and the Appendix for $n = 2$). As a consequence, there is a near-cancellation of

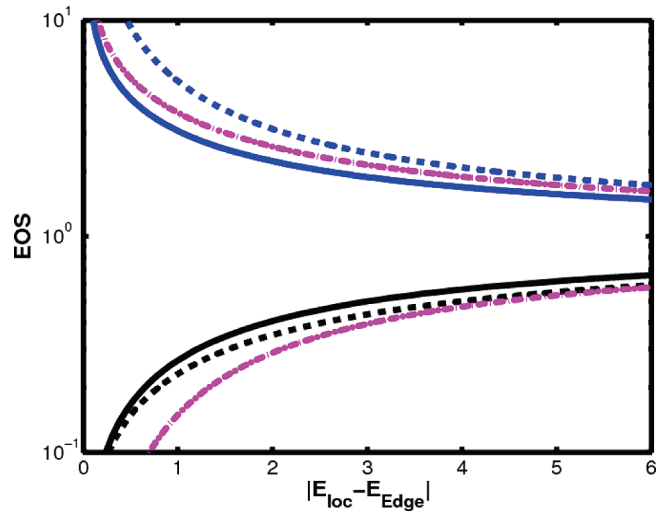

Figure 4. Effective oscillator strength (EOS) vs energy of the localized states relative to the bottom of the band. The upper three curves are associated with normal bands; the lower three curves with inverted bands. Solid curve, $n = 3$; dashed curve, $n = 2$; broken curve, nearest-neighbor transfer. Energy is in units of the nearest-neighbor transfer integral. Data displayed in nearest-neighbor curves are obtained from eq 13.

the sum in eq 12 when the localized state associated with an inverted band is near the bottom of the band, whereas in the normal-band case the amplitudes add in phase.[6,7]

As mentioned in the Appendix, because of the quadratic variation in the exciton energy near the bottom of the band in inverted-band systems with $n \geq 2$ and in normal-band systems when $n > 3$, the asymptotic amplitudes of the localized states decay exponentially with distance from the perturbed site. This behavior can be made more explicit by considering the amplitude equations in the quadratic approximation:

$$g_j(\Lambda) = -\pi^{-1} \int_0^{\pi} \mathrm{d}k \cos(jk)/[\Lambda + D_{\mathrm{inv}}(n)(\pi - k)^2] \tag{18}$$

for inverted-band systems and

$$g_j(\Lambda) = -\pi^{-1} \int_0^{\pi} \mathrm{d}k \cos(jk)/[\Lambda + D(n)k^2] \tag{19}$$

for normal-band systems, where in both cases $\Lambda = E_{\mathrm{edge}} - E_{\mathrm{loc}}$. The asymptotic behavior is obtained by extending the limits of integration to infinity (after making the variable change $y = \pi - k$ in the inverted-band case) with the results

$$g_j(\Lambda) = -(4D_{\mathrm{inv}}(n)\Lambda)^{-1/2} \cos(j\pi) \exp[-|j|(\Lambda/D_{\mathrm{inv}}(n))^{1/2}] \tag{20}$$

for inverted bands and

$$g_j(\Lambda) = -(4\Lambda D(n))^{-1/2} \exp[-|j|(\Lambda/D(n))^{1/2}] \tag{21}$$

for normal bands. In eqs 20 and 21, the appropriate values of $D_{\mathrm{inv}}(n)$ and $D(n)$ are $D_{\mathrm{inv}}(2) = {}^1/_2$, $D_{\mathrm{inv}}(3) = \ln(2)$, $D_{\mathrm{inv}}(n > 3) = (1 - 2^{3-n})\zeta(n - 2)$; $D(n) = \zeta(n - 2)$ $(n > 3)$. In the large-n limit both $D_{\mathrm{inv}}(n)$ and $D(n)$ approach 1, the value for nearest-neighbor transfer with $T_{jj+1} = 1$. It should be noted when the

exciton energy displays quadratic behavior, the localized state energy at small ε also involves D or D_{inv}; we have $E_{loc} \approx E_{edge} - \varepsilon^2/D^*(n)$ where $D^*(n) = D(n)$ or $D_{inv}(n)$, as appropriate.

We have also investigated the case normal band with $n = 3$ where the exciton energy varies as k^2 [3/2 − ln(k)] as $k \rightarrow 0$.[9] Evaluating the integral in eq 5 numerically and then fitting the result to a power law over the interval $0.005 \leq |E_{loc} - E_{edge}| \leq 0.05$, we obtain the approximate behavior $E_{loc} \approx E_{edge} - 0.78\varepsilon^{2.5}$.

IV. Discussion

In this article, we have investigated localized states in 1D Frenkel exciton chains that were created by a downward shift in the optical transition frequency of a single chromophore. In the analysis, a comparison was made between localized states in chains with nearest-neighbor transfer and localized states in chains with infinite-range transfer. A distinction was also made between normal bands where the state with $k = 0$ is at the bottom of the band and inverted bands where the $k = \pi$ state is lowest in energy. Similarities and differences between the results for nearest-neighbor and infinite range transfer in normal and inverted band systems are pointed out and analyzed. In the case of the participation ratio, the localized states in both normal and inverted bands showed qualitatively similar behavior, rapidly increasing as the separation from the band edge went to zero.

With respect to the experimental implications of the work, one of the more interesting findings is the difference in the effective oscillator strengths between localized states below the band edge in normal and inverted band systems. As noted, the EOS for localized states in inverted band systems is significantly smaller than that in normal band systems at a given energy below the band edge for both nearest-neighbor and infinite range transfer. As a consequence, optical absorption and fluorescence associated with these states is much weaker than that in the normal case, all else being equal. It should be noted that the enhanced optical activity of localized normal-band exciton states with energies near the band edge was originally predicted for Mott−Wannier excitons by Rashba and Gurgenishvili[10] and subsequently observed in CdS by Henry and Nassau.[11]

An area of current interest where the results of this article may be useful in interpreting the optical data is the polyfluorenes (PF) and in particular poly(di-*n*-octylfluorene) (PF8). PF8 is unusual in that it has been shown that the states giving rise to the blue photoluminescence in the β phase are extended and can be characterized by a Frankel exciton model with nearest-neighbor interactions.[12] Depending on sample preparation, the luminescence spectra of the PF can also have a green component that is associated with ketonic defects that is located approximately 0.5 eV below the bottom of the exciton band.[13,14] In the β phase of PF8, the nearest-neighbor transfer integral is equal to 1.35 eV j[12] so the corresponding localized state energy, relative to the center of the band, is −2.4 in units of the transfer integral.[7] The corresponding participation ratio, calculated from eq 10, is 2.8 indicating that the state, while localized, has significant amplitude on more than one site. It should be noted that this value most likely represents an upper limit for the PR because it is obtained assuming that the transfer integral between the defect and the host monomer is the same as the transfer integral coupling monomers.

Appendix

In this appendix, we investigate the asymptotic behavior of the localized mode amplitudes for the model presented in section III A. We begin with the inverted band where the exciton energy is equal to $-\pi^2/6 + (k - \pi)^2/2$. Apart from a normalization factor, the amplitude of the localized mode at the site n is given by the integral

$$g_j(E_{loc}) = \pi^{-1} \int_0^{\pi} dk \cos(jk)/[E_{loc} + \pi^2/6 - (k - \pi)^2/2] \quad (A1)$$

Writing $E_{loc} = -\pi^2/6 - \Lambda$ ($\Lambda > 0$) and letting $y = j(\pi - k)$, A1 becomes

$$g_j(\Lambda) = -(2j/\pi)\cos(j\pi) \int_0^{j\pi} dy \cos y/[2j^2\Lambda + y^2] \quad (A2)$$

The asymptotic form is obtained by extending the integral to infinity, with the result

$$g_j^{asymp}(\Lambda) = -(2\Lambda)^{-1/2}\cos(j\pi)\exp[-|j|(2\Lambda)^{1/2}] \quad (A3)$$

showing exponential decay with oscillating sign similar to the asymptotic behavior of the inverted band with nearest-neighbor transfer.

In the case of the normal band, the amplitude on site j is proportional to the Green's function

$$g_j(E_{loc}) = \pi^{-1} \int_0^{\pi} dk \cos(jk)/[E_{loc} - \pi^2/6 + (k - \pi)^2/2] \quad (A4)$$

Writing $E_{loc} = -\pi^2/3 - \Delta$ ($\Delta > 0$) and letting $y = j(\pi - k)$, g_j can be written

$$g_j(\Delta) = -(2j/\pi)\cos(j\pi) \int_0^{j\pi} dy \cos y/[j^2(\pi^2 + 2\Delta) - y^2] \quad (A5)$$

Focusing attention on localized states near the bottom of the exciton band, where $2\Delta/\pi^2 \ll 1$, and noting the dominant contribution to the integral when $j \gg 1$ comes from the region near the upper limit, we make the variable transformation $u = (j\pi - y)$ and obtain the result

$$g_j(\Delta) = -(2j/\pi) \int_0^{j\pi} du \cos u/[j^2(\pi^2 + 2\Delta) - (u - j\pi)^2] \quad (A6)$$

The leading contribution to this integral is from the region $u \approx 0$. Neglecting u^2 in the denominator and making the variable change, $x = (\pi/j\Delta)u$, we obtain

$$g_j(\Delta) \approx -\pi^{-2} \int_0^{\pi^2/\Delta} dx \cos(jx\Delta/\pi)/[1 + x] \quad (A7)$$

Because $\pi^2/\Delta \gg 1$, we extend the upper limit to infinity. The resulting integral can be expressed in terms of the real part of an expression involving the exponential integral E_1 with the imaginary argument $-ij\Delta/\pi$[15]

$$g_j(\Delta) = -\pi^{-2}\mathrm{Re}(\exp[-ij\Delta/\pi]E_1(-ij\Delta/\pi)) \quad (A8)$$

Using the asymptotic expansion of E_1, we obtain the asymptotic amplitude

$$g_j^{\text{asymp}}(\Delta) = -(j\Delta)^{-2} \tag{A9}$$

which is seen to decay algebraically rather than exponentially as is the case with the inverted band. Note that in eq A9 terms of order $(j\pi^2)^{-2}$ are neglected, consistent with the assumption $\Delta/\pi^2 \ll 1$.

We note that the asymptotic exponential decay of the site amplitudes found for the inverted band is a direct consequence of the fact that the exciton energy varies quadratically with $\pi - k$ in the long wavelength limit when the band is inverted. The quadratic variation is present in inverted bands for $n = 2$, 3, ... and in normal bands with $n > 3$.[9] As a result, the asymptotic exponential decay is a feature of inverted-band systems with $n \geq 2$ as well as normal-band systems with $n > 3$. The behavior of the normal band system with $n = 3$ is expected to be nearly exponential because the exciton energy is quadratic with a logarithmic correction.[9]

References and Notes

(1) Agranovich, V. *Excitations in Organic Solids*, International Series of Monographs in Physics 142; Oxford University Press: London, 2009; Chaps. 2 and 3.

(2) Koster, G. F.; Slater, J. C. *Phys. Rev.* **1954**, *95*, 1167–1176, ibid. 96 1208−1233.

(3) Montroll, E. W.; Potts, R. B. *Phys. Rev.* **1955**, *100*, 525–543.

(4) Mahanty, J.; Maradudin, A. A.; Weiss, G. H. *Progr. Theoret. Phys. (Kyoto)* **1958**, *20*, 369–394.

(5) Wolfram, T.; Callaway, J. *Phys. Rev.* **1963**, *130*, 2207–2217.

(6) Avgin, I.; Winokur, M.; Huber, D. L. *J. Lumin.* **2007**, *125*, 108–111.

(7) Avgin, I.; Huber, D. L. *Proceedings of the 2008 International Conference on Luminescence, J. Lumin*. (available electronically from Elsevier through the link doi:10.1016/j.jlumin.2009.03.038).

(8) Gradshteyn, I. S.; Ryzhik, I. M. *Tables of Integrals, Series, and Products*, 4th edition; Academic Press: Orlando, 1980; Chap. 1, p 39.

(9) Malyshev, V.; Moreno, P. *Phys. Rev. B* **1995**, *51*, 14587−14593.

(10) Rashba, E. I.; Gurgenishvili, G. E. *Fiz. Tverd Tela* **1962**, *4*, 10. Eng. Trans. *Sov. Phys.−Sol. State* 1962 *4*, 759−760. See also Toyozawa, Y. *Optical Processes in Solids* Cambridge University Press: Cambridge, 2003; Chap. 8, p 141.

(11) Henry, C. H.; Nassau, K. *J. Lumin.* **1970**, *1−2*, 299–306.

(12) Chunwaschirasiri, W.; Tanto, B.; Huber, D. L.; Winokur, M. J. *Phys. Rev. Lett.* **2005**, *94*, 107402−1107402−4.

(13) Lupton, J. M.; Craig, M. R.; Meijer, E. W. *Appl. Phys. Lett.* **2002**, *80*, 4489–4491.

(14) List, E. J. W.; Guenter, R.; Scanducci de Freitas, P.; Scherf, U. *Adv. Mater.* **2002**, *14*, 374−378.

(15) Abramowitz, M.; I. A. Stegun, I. A. *Handbook of Mathematical Functions* Dover Publications: New York, 1972; Chap. 5, p 230.

JP9061863